Developments in the Material Fabrication and Performance of $LiMn_2O_{4-d}Cl_d$ Cathode Material

Paula C Latorre, Ashley L Ruth, and Terrill B Atwater
U.S. Army RDECOM
Communications, Electronics, Research, Development and Engineering Center
Aberdeen Proving Ground, MD 21005

Abstract: *Lithium manganese oxide spinel materials exhibit promising electrochemical performance and good thermodynamic and kinetic stability when used as a cathode in lithium and lithium-ion electrochemical systems. An inherent disadvantage is their limited cyclability as a result of the energy barriers for removing lithium from the octahedral sites. This work incorporates chlorine into the lattice of the AB_2O_4 to help assist in lithium deinsertion from the octahedral sites. By introducing this chlorine into the starting material and the subsequent final product, the overall electrochemical performance is enhanced, which will be extremely useful in versatile applications. $AB_2O_{4-d}Cl_d$ materials were synthesized using both a solid state reaction method and a common ceramic glycine nitrate combustion process and were evaluated as a cathode for lithium and lithium-ion electrochemical systems. The data presented in this paper is the result of continuing fabrication efforts that allow for an even distribution of chlorine in the $AB_2O_{4-d}Cl_d$ material lattice. The material properties were verified using X-ray diffraction and X-ray fluorescence to determine the extent of chlorination into the lithium manganese spinel mixture. Electrochemical coin cells were fabricated and cycled between 4.75 V and 3.5 V at 1-2 mA/cm^2 to determine cycle life capability and degradation processes.*

Keywords: Lithium manganese spinel; Lithium rechargeable batteries, Lithium-ion battery

Introduction

As portable electronic systems continue to advance in both complexity and capability, so does the need for an advanced portable power device that can meet the demands of current and future portable electronic systems. In the U.S. Army, many of these systems are utilized in a Command, Control, Communication, Computers, Intelligence, Surveillance, and Reconnaissance (C4ISR) environment, where the system must be capable of consistent operation for an allotted period of time. Therefore, the system's portable power device must also have equivalent operational reliability and safety requirements. Lithium and lithium-ion battery systems are highly sought after for rechargeable applications due to their high energy density (Wh/L) and high specific energy (Wh/kg), specifically to meet the rigorous requirements placed on them for operational field use. Lithium manganese oxide spinel ($LiMn_2O_4$) is a potential viable active cathode material for use in these versatile applications due to its low toxicity, good capacity, and low cost.

Background

Lithium oxide spinels are plagued by capacity fading, where a cell loses cycle capacity over the duration of its useable life. Capacity fading limits the cell's number of practical cycles, which in turn decreases the overall system availability once integrated into a product. In lithium battery systems, capacity loss is attributed to degradation in the active cathode material due to constant cycling. Degradation of the active material can be due to loss of crystallinity, alternative phase formations, or potential side reactions.[1-4] Methods to eliminate or mitigate this degradation effect include changing the crystal structure and composition of the active material.

Some studies have incorporated chlorine or fluorine into the starting material and have reported positive impacts on the active material's electrochemical performance.[5-7] However, the halide is not reported to be incorporated into the lattice structure. These studies used the standard processing method for lithium manganese oxide spinels and demonstrated an increase in capacity. However, capacity retention issues in regard to cycle life were observed between cycles 10 to 20.[6,7]

Our group has utilized two different processing methods to successfully introduce chlorine into the starting material and subsequently into the final product, enhancing the material's electrochemical performance. The first method involves a solid state process in which the anion, either fluorine or chlorine, is incorporated into the material.[8] This method has yielded active material which has previously reported cyclability to 20 cycles.[9-11] The second processing method incorporates chlorine into the bulk of the lithium spinel material via in-situ combustion synthesis. This paper will focus on the discussion and evaluation of both processing methods and their effect on cycle life performance.

Experimental

The active cathode material, $Li_xMn_2O_{4-d}Cl_d$, was fabricated using two different processing methods. The first

processing method involved a reduced solid state process (SSP) where starting materials included MnO_2, Mn_2O_3, or Mn_3O_4, Li_2CO_3 or LiOH, and a halide salt, such as $LiClO_4$. The starting material mixture was grinded in a mortar and pestle until uniform. The subsequent mixture was then placed in an orbit mixer mill for one hour and then calcined in air at 600 °C for at least two hours. Multiple samples of the final material, $Li_xMn_2O_{4-d}Cl_d$, was produced with varying concentrations of the halide salt in order to determine the extent of halide retention in the crystal structure. The second material fabrication method used in this paper was a glycine nitrate combustion process (GNP) to synthesize $Li_xMn_2O_{4-d}Cl_d$. Lithium nitrate, along with hydrated manganese nitrate and halide salt (manganese chloride) were dissolved in deionized water. Glycine was then added to the aqueous solution as a chelating agent. The subsequent solution was then heated until the water fully evaporated. The resultant gel was then heated until auto ignition occurred, forming a black ash. Ash was then collected and grinded in a mortar and pestle until uniform. The material was then calcined in air at 600 °C for at least two hours. Both calcined final materials were then evaluated for their viability as cathode materials for rechargeable lithium batteries.

In order to determine if any structural changes occurred in each sample, a baseline material ($LiMn_2O_4$) was fabricated using a traditional sol-gel method. XRD and XRF were used to analyze and compare the structure of the resultant baseline material with $Li_xMn_2O_{4-d}Cl_d$ materials formed using both the SSP and GNP mentioned previously. Additionally, these three materials (prior to calcination) were also evaluated using thermogravimetric analysis (TGA) to observe the reaction thermodynamics.

Coin cells were fabricated using a lithium anode, an organic electrolyte, and a cathode using the $Li_xMn_2O_{4-d}Cl_d$ material to evaluate the thermodynamic and kinetic properties of the resultant $Li//Li_xMn_2O_{4-d}Cl_d$ electrochemical system. The lithium anode consisted of lithium foil that was approximately 0.075 cm thick and was cut using a 12.7 mm diameter hole punch. The cathode material consisted of $Li_xMn_2O_{4-d}Cl_d$, carbon black, and polytetrafluoroethylene (PTFE) in a ratio of 85:10:5. The cathode was cut into 1.0 cm^2 discs which were approximately 0.1 to 0.15 g. The anode and cathode were separated using a 0.01 cm nonwoven glass separator. The electrolyte medium used was a 1 molar solution of $LiPF_6$ with proportional mixtures of diethyl carbonate, dimethyl carbonate, and ethylene carbonate.

The electrochemical coin cells were cycled using an ARBIN MSTAT4 battery cycler system controlled by MITS pro software. The cells were discharged and charged from 4.75 V to 3.5 V at a rate of 1 mA/cm^2 to evaluate capacity retention. A 15-minute rest was introduced between charge and discharge cycles to allow for cells to reach equilibrium. Data was logged every 15 minutes or every 0.01 V during both charge and discharge.

Results

After the final active materials were fully calcined, their physical properties were evaluated using X-ray diffraction (XRD). Figure 1 shows the diffraction patterns of $Li_xMn_2O_{4-d}Cl_d$ formed using both SSP and GNP, shown as "b" and "c" respectively, where $x \approx 1$ and $d \sim 0.05$. The traditional $LiMn_2O_4$ spinel diffraction pattern is also shown for comparison. The peaks presented in each pattern correlate directly with the JCPDS file for $LiMn_2O_4$ spinel (00-018-0736). The lack of additional peaks indicate the achievement of a single phase spinel.

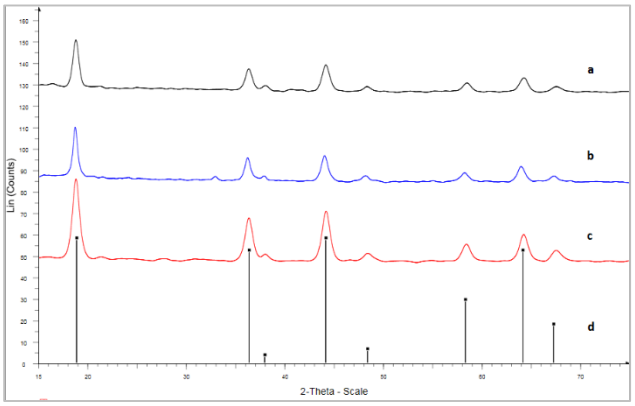

Figure 1. XRD patterns of $LiMn_2O_4$ (a), $Li_xMn_2O_{4-d}Cl_d$ made by SSP method (b), and $Li_xMn_2O_{4-d}Cl_d$ made by GNP method (c), along with JCPDS file for $LiMn_2O_4$ (d).

X-ray fluorescence (XRF) spectroscopy was also performed on all post-calcined materials to determine and characterize the elemental components of the material. Figure 2 shows the XRF results of $Li_xMn_2O_{4-d}Cl_d$ formed using both SSP and GNP. The figure shows similar material compositions with the exception of a peak intensity divergence at 2.63 keV. Peak intensities at this energy are 5206 and 2016 A.U. for $Li_xMn_2O_{4-d}Cl_d$ spinels made by SSP and GNP, respectively. These peaks correlate to the corresponding energy for chlorine, indicating a retention of Cl present in the sample after calcining. The Si, P, and S present in each sample are attributed to the sample holder, and Pd is from the X-ray source.

A series of $Li_xMn_2O_{4-d}Cl_d$ spinels were made via SSP, where $x \approx 1$ and $0.025 < d < 0.15$, to determine the extent of chlorine doping in the material through XRF. Figure 3 shows the weight percent of Cl in the sample prior to and after calcining the material. In each sample, the pre-calcination value of Cl is greater by approximately 50%.

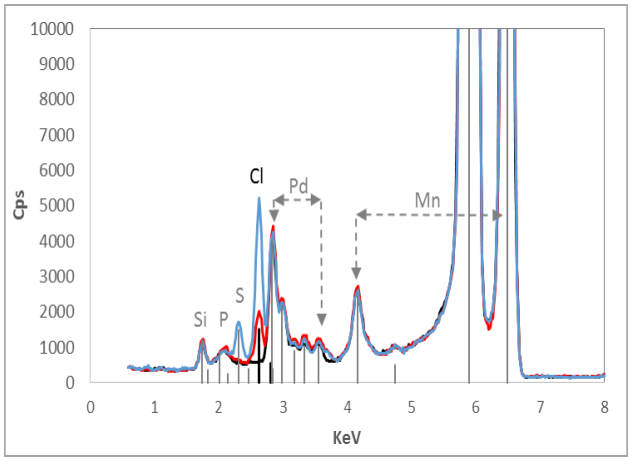

Figure 2. XRF of $LiMn_2O_4$ (black), $Li_xMn_2O_{4-d}Cl_d$ made by SSP method (blue), and $Li_xMn_2O_{4-d}Cl_d$ made by GNP (red).

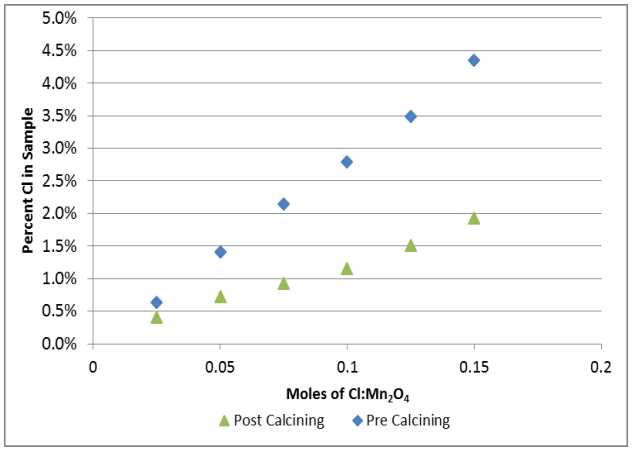

Figure 3. Weight percent of chlorine present in each sample before and after calcining using SSP method.

TGA was performed to determine the appropriate temperature of calcination for each process as well as the thermodynamics of the reaction. Figure 4 shows the resultant weight percent TGA curve for $Li_xMn_2O_{4-d}Cl_d$ spinel precursors using both processing methods. The TGA was performed in air from 30 °C to 750 °C at a rate of 10 °C/min. The dehydration of water molecules, which occurred between 30 and 100 °C, amounted to a 5% mass decrease, which was then normalized in the figure for the GNP process (shown in red). The calcining temperature of 600 °C could potentially be reduced, as the slow mass loss after 400 °C in the SSP material and 500 °C in the GNP material is probably attributed to Cl evolution. The figure demonstrates the comparative standard composition and formation of the spinel.

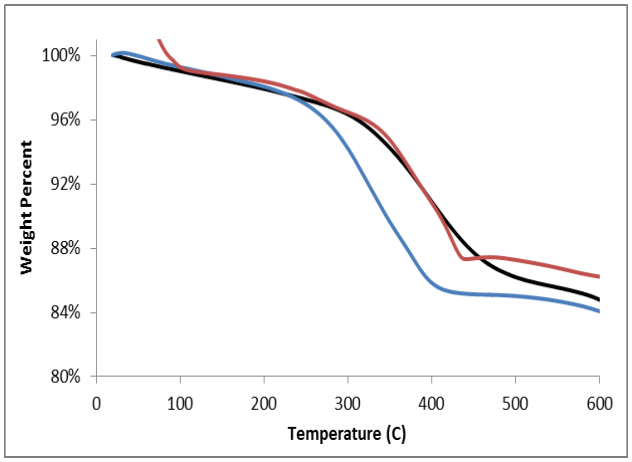

Figure 4. TGA of precursors of $LiMn_2O_4$ (black), $Li_xMn_2O_{4-d}Cl_d$ made by SSP method (blue), and $Li_xMn_2O_{4-d}Cl_d$ made by GNP (red) normalized to eliminate weight reduction due to water loss.

After material analysis was performed, the $Li_xMn_2O_{4-d}Cl_d$ spinel was utilized as the active cathode material in a $Li//Li_xMn_2O_{4-d}Cl_d$ electrochemical coin cell. Figure 5 shows the differential capacity of a representative cell, where the active material was made via GNP. Cells were cycled in their reversible region, between 4.75 V and 3.5 V[10-12]. The figure shows minimal IR shifts up until cycle 100, after which the features begin to slowly degrade, specifically the low voltage peak centered at 4.0 V. Degradation may be attributed to either conductivity or kinetic changes in the cell, leading to a lower coulombic efficiency.

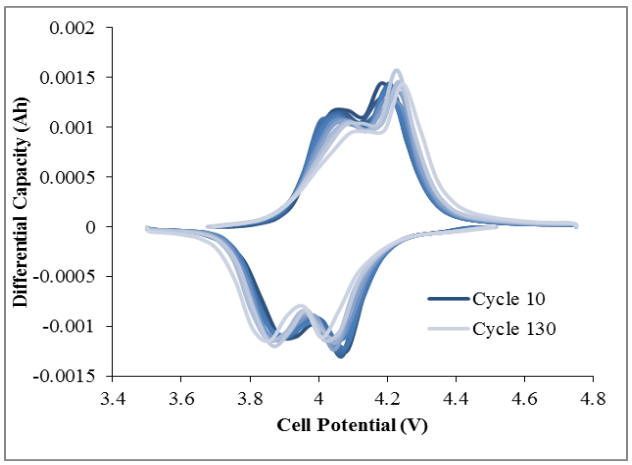

Figure 5. Differential capacity for a $Li//Li_xMn_2O_{4-d}Cl_d$ electrochemical cell made by GNP displaying 130 cycles.

Cycle life data of electrochemical cells were compared at varying degrees of Cl content present in the active material. The specific capacity for each cycle of three variant cells is shown in Figure 6. The first cell (depicted as "c") was made using the SSP process to produce $Li_xMn_2O_{4-d}Cl_d$ spinel, where $x \approx 1$and $d \approx 0.025$. The second cell (depicted

as "b") was alternatively made using the GNP process to produce $Li_xMn_2O_{4-d}Cl_d$ spinel, where x ≈ 1 and d ≈ 0.045. Both of these cells demonstrate good cycle life with overcharge beginning to occur at cycle 100, which begins to impact the cell's performance. However, the cells are still able to retain 95% of their original capacity after 130 cycles. Comparatively, the third cell (depicted as "a") was made using the SSP process to make $Li_xMn_2O_{4-d}Cl_d$ spinel, where x ≈ 1and d ≈ 0.05. Cell "a" shows a decrease in capacity retention and cycle life, although it had the highest initial specific capacity at approximately 0.10 Ah/g. Cycles 39-48 were omitted due to shorting. Although the cell suffered significant shorting and capacity loss for 10 cycles, it was able to recover.

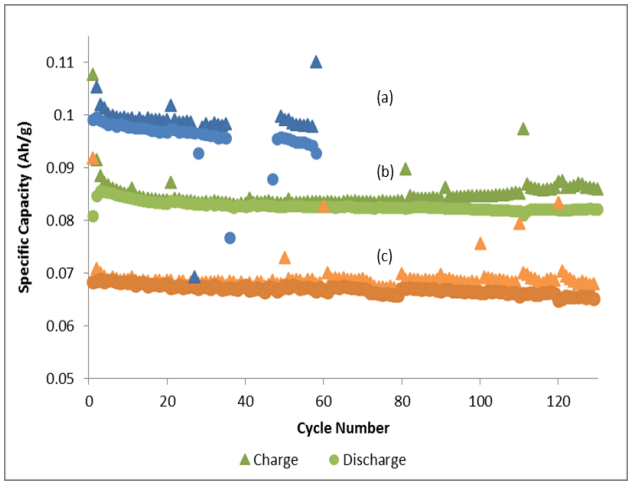

Figure 6. Specific capacity for Li//$Li_xMn_2O_{4-d}Cl_d$ electrochemical cells where d ≈ 0.050 (a), d ≈ 0.045 (b), and d ≈ 0.025 (c).

These cells show a clear correlation between cycle life, specific capacity, or capacity retention and the amount of Cl present in each sample. Cells fabricated with decreasing values of Cl present have a longer cycle life and better capacity retention, at the expense of their nominal specific capacity. Alternatively, cells fabricated with higher Cl content present in the sample have a higher specific capacity with limited cycle life. However, these three cells were fabricated using different processing methods, two using SSP and the third using GNP. Further studies would have to be performed in order to conclude if the processing method had any additional impact on the cells' electrochemical performance. Additionally, these cells were cycled at high voltages and the electrolyte utilized may be insufficient at high voltage, causing the cell to fail prematurely.

Conclusions

Chlorine-doped lithium manganese oxide spinel was synthesized using two processing methods: a reduced solid state process and a glycine nitrate combustion process. Both of these processing methods drastically reduced the manufacturing cost and time to produce a single phase $LiMn_2O_4$ spinel material. Formation of a single phase material was confirmed via X-ray diffraction and Cl was verified to remain in the sample after calcination via X-ray fluorescence, although some Cl was lost during processing. Thermogravimetric analysis verified the proper thermodynamics during calcining to produce lithium manganese oxide spinel in all samples. $Li_xMn_2O_{4-d}Cl_d$ spinel was incorporated into the cathode of electrochemical coin cells paired with lithium metal. The coin cells demonstrate a correlation between cell performance and Cl present in the cathode material. Cells with lower Cl doping show good cycle life retention even when overcharging. Further testing and evaluation is recommended to evaluate high voltage electrolytes in order to mitigate capacity degradation. With further optimization, the robust LixMn2O4-dCld spinel materials will be promising active materials for future integration into lithium-ion batteries.

References

1. Reddy, Thomas B. *Linden's Handbook of Batteries*. Vol. 4. New York: McGraw-Hill, 2011.
2. Xia, H., Z. Luo, and J. Xie, *Progress in Natural Science*, vol. 22, pp. 572, 2012
3. Huang, H., C. A. Vincent, P. G. Bruce, *Journal of the Electrochemical Society*, vol. 146, pp. 3649, 1999
4. Xia, H. and M. Yoshio, *Journal of the Electrochemical Society*, vol. 143, pp. 825, 1996
5. Amatucci, G.G., N. Pereira, T. Zheng, I. Plitz, and J.M. Tarascon, *Journal of Power Sources*, vol. 81, pp. 39, 1999
6. Liu, W.R., S.H. Wu, and H.S. Sheu, *Journal of Power Sources*, vol. 146, pp. 232, 2005
7. Son, J.T., and H.G. Kim, *Journal of Power Sources*, vol. 147, pp. 220, 2005
8. Atwater, T. B., and P. C. Tavares, **US Patent No. 8,597,377**, December 3, 2013
9. Atwater, T. B., and P. C. Tavares, PC, **US Patent No. 8,900,756**, December 2, 2014
10. Atwater, T. B., and P. C. Tavares, *Proceedings of the 45th Power Sources Conference*, 2012
11. Atwater, T. B. and Latorre, P. C., *SAE Int. J. Materials and Manufacturing*, Vol. 6, no. 1,pp. 85-89, 2013
12. Atwater, T. B., and P. C. Latorre, *Proceedings of the 46th Power Sources Conference*, 2014
13. Amine et al, **US Patent No. 5,677,087**, October 14, 1997